STUDIA UBB CHEMIA, LXI, 3, Tom I, 2016 (p. 195-214)
(RECOMMENDED CITATION)

Dedicated to Professor Luminița Silaghi-Dumitrescu on the occasion of her 65th anniversary

PHYSICO-CHEMICAL PROPERTIES AND CRYSTAL VIOLET ADSORPTION PERFORMANCES OF H_3PO_4 - MODIFIED MANGO SEEDS KERNEL

GHISLAIN ARNAUD MOUTHE ANOMBOGO[a,b,c], ANDRADA MĂICĂNEANU[b,*], JEAN BAPTISTE BIKE MBAH[a], CHRISDEL CHANCELICE NDJEUMI[a,b,c], LIVIU COSMIN COTEŢ[b], RICHARD KAMGA[a]

ABSTRACT. This study investigated the removal of Crystal Violet (CV) from aqueous solutions using H_3PO_4-modified mango seeds kernel (H_3PO_4-MSK). The adsorbent was characterized using elemental analysis, thermal analysis (TGA), scanning electron microscopy (SEM), specific surface area and pore size distribution (BET) and Fourier Transformed Infrared Analysis (FTIR). X-ray diffraction (XRD) analysis showed that H_3PO_4-MSK is a type II cellulose crystal structure, while SEM and BET analysis confirmed the macroporosity of the adsorbent. The removal efficiency of CV increased with an increase in adsorbent quantity and temperature. The adsorption capacities increased from 23.94 to 87.23 mg/g for an increase in temperature from 30 to 50°C. Adsorption kinetics analysis indicated that pseudo-second-order and Elovich equations fitted very well the adsorption of CV onto H_3PO_4-MSK. The adsorption process followed the Temkin and Langmuir isotherm models. Isotherm modelling showed that CV is loosely bound to H_3PO_4-MSK. Further thermodynamic analysis revealed that the removal of CV from aqueous solution by H_3PO_4-MSK was a spontaneous and endothermic process. The proposed adsorption mechanism involves -OH, $-NH_2$ and -COOH groups from the H_3PO_4-MSK surface.

***Key words**: H_3PO_4-modified mango seeds kernel, adsorption, Crystal Violet, kinetics, equilibrium, thermodynamics*

[a] *Laboratoire des Matériaux et Chimie Industrielle Inorganique, National Advanced School of Agro-Industrial Sciences, University of Ngaoundere, P.O. BOX 455 Ngaoundere, Cameroon.*
[b] *Department of Chemical Engineering, Babeş-Bolyai University, 11 Arany Janos st.,Cluj-Napoca, RO-400028, Romania.*
[c] *Department of Environmental Sciences, Higher Institute of the Sahel, University of Maroua, P.O. BOX 46 Maroua, Cameroon*
**Corresponding author: andrada@chem.ubbcluj.ro*

INTRODUCTION

Contamination of water is a worldwide environmental concern. This contamination is generated by urbanization, agriculture and industries, and particularly, in case of dyes, textile industries [1]. Textile industry is one of the main industries in Cameroon. This industry produces a large amount of wastewater which contain high amount of coloring dyes. Many methods have been developed to remove organic and inorganic pollutants from water. They include coagulation-flocculation [2,3], chemical oxidation [4-6], adsorption [7-9], etc. Among these methods, adsorption is considered to be easy to use, low cost and with high efficiency in wastewater treatment [7,8].

Many adsorbents have been used for the removal of undesirable substances from aqueous solution [10-13]. Among these adsorbents, activated carbon is found to be the most efficient. However, the high cost of production and of regeneration of activated carbon limits its use as adsorbent and encourage its substitution by low cost materials. Recent studies have demonstrated that a wide variety of low cost adsorbents, such as agricultural residues, can be employed, with minimum treatment, as biosorbents for the removal of organic and inorganic pollutants from wastewaters [14-16]. The implication of untreated fruit and vegetable wastes as adsorbents tends to generate several problems such as low adsorption, high Chemical Oxygen Demand (COD) and Biochemical Oxygen Demand (BOD) as well as total organic carbon due to release of soluble organic compounds from the plant materials, which eventually leads to depletion of oxygen content in water and threaten aquatic life. Therefore, plant wastes need to be modified or treated prior to their use in water purification. Chemical modifications involve treatment of the adsorbents with an array of chemicals for the elimination of undesired substances, enhancement of binding groups, elimination of inhibiting groups and graft copolymerization [17].

A recent study indicated that mango leaves, pits, seeds and husks are potential adsorbents for the removal of dyes from aqueous solutions [18-22]. Cameroon is an important producer of mango (*Mangifera Indica*) in Central Africa Region [23, 24] and the waste residues of this fruit are abundant. These residues can be used with minimum treatment as adsorbent for textile dye removal from aqueous solution. The purpose of this work was to study the physico-chemical characteristics of H_3PO_4-modified mango seeds kernel (Kent specie), H_3PO_4-MSK, and their use for the removal of Crystal Violet (CV) from aqueous solution.

2. RESULTS AND DISCUSSION

Physico-chemical characterization of H_3PO_4-MSK

Elemental analysis. Carbon, hydrogen nitrogen and oxygen content of the H_3PO_4-MSK were determined to be as follows C: 56.03%, H: 5.21%, N: 2,53% and O: 36.23%. These values are similar to those usually found in lignocellulosic materials [18,25,26].

Thermal analysis. The TG curve for H_3PO_4-MSK showed three distinct patterns of weight loss (Fig. 1). In the temperature range of 25 to 160°C there is a gradual weight loss, in the range of 160 to 900°C there is a steep weight loss and a continuous decrease of weight is observed at temperature higher than 900°C. Associated numerical values of these weight losses are presented in Table 1. DTG curve showed two main endothermic peaks. The first peak between 25 and 160°C corresponds to the H_3PO_4-MSK powder dehydration. The second peak between 160°C and 900°C with a maximum at 372°C is an overlapping peak with two shoulders observed at 240°C and 320°C. Many phenomena are associated to this second peak. These phenomena could be evaporation of water condensed in the pores, evaporation of volatile organic compounds, dehydroxylation and degradation of H_3PO_4-MSK powder. The peak at 372°C could be associated with the degradation of cellulose, while those appearing at 240 and 320°C could be associated to the degradation of starch and lignin respectively [18,20].

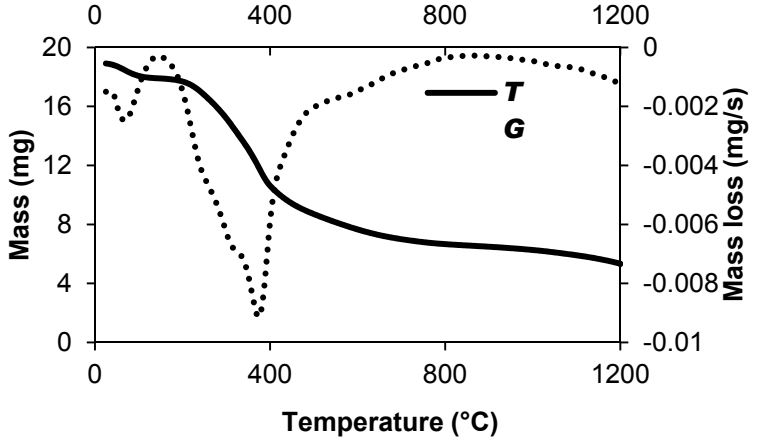

Figure 1. TG and DTG graphs of H_3PO_4-MSK.

Table 1. Thermogravimetic and derivative analysis (TG and DTG) of H_3PO_4-MSK.

Amount (mg)	**Total mass loss** (%)	**Temperature interval** (°C)	**Partial mass loss** (%)	**T_{max}** (°C)
18.91	71.4	25 - 160	5.2	67
		160 - 900	60.3	372
		900 - 1200	5.9	Continuous

Structural analysis. SEM micrographs of H_3PO_4-MSK are presented in Fig 2. Images showed a lamellate structure (Fig 2a) and a heterogeneous surface of the H_3PO_4-MSK sample (Fig 2b).

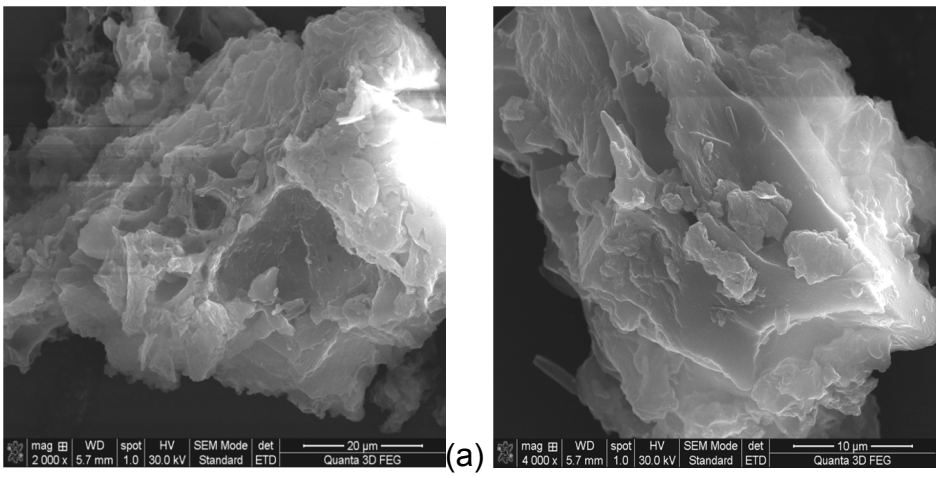

Figure 2. SEM micrographs of H_3PO_4-MSK.

Morpho-structural properties of H_3PO_4-MSK. The specific volume and specific surface area values of H_3PO_4-MSK are 10.24 cm^3/g and the BET surface 44.57 m^2/g, respectively.

XRD analysis. The XRD studies showed that the apparently amorphous material presents a crystalline structure even if it does not present properties like angle and crystal face usually associated to the crystal structure [27]. The diffraction patterns of H_3PO_4-MSK exhibited a mixture of polymorphs I and cellulose II, with a remarkable predominance of type II cellulose (Fig. 3). The

presence of type II cellulose is reflected by peaks at 2θ =19.40° (plane 100) and 21.57° (plane 002) [28]. Reticular distances were 4.57 and 4.11 Å, respectively. The presence of type II cellulose in this work is associated with the regeneration of cellulose after hydrolysis.

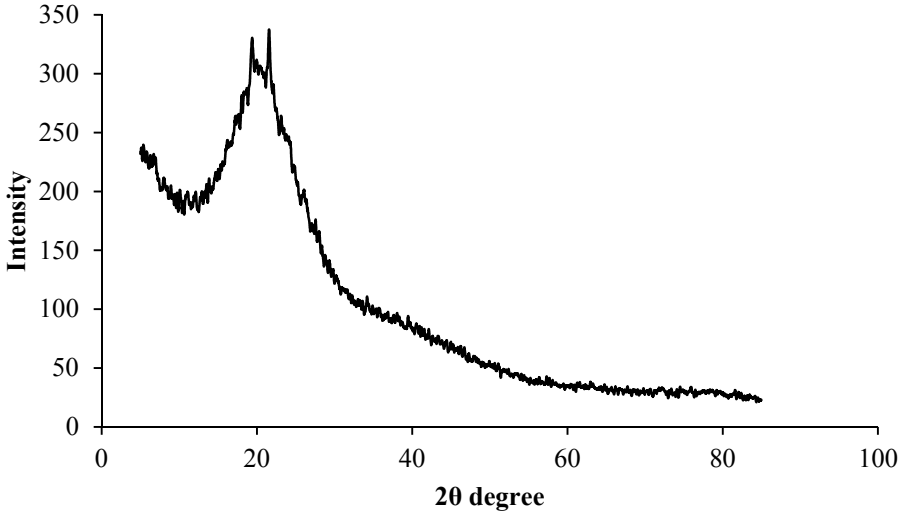

Figure 3. XRD diffractogram of H_3PO_4-MSK.

Surface chemistry. The FTIR spectral analysis is important to identify the different functional groups of the adsorbent surface. Peaks appearing in the FTIR spectrum of MSK (Fig. 4a) and H_3PO_4-MSK (Fig. 4a) were assigned to various chemical groups and bonds in accordance with their respective wavenumber as reported in the literature. The FTIR spectral of MSK and H_3PO_4-MSK are very similar. However, at low wavelengths (<1800 cm^{-1}) the spectra of MSK, have its peaks more intense than those of H_3PO_4-MSK ones. This difference can be attributed to the presence of hydrogen bonds among substances present in the crude mango seeds kernel. H_3PO_4 treatment of mango seeds leads to the removal of some fatty acids compounds and to the rupture of some H-bonds. The region at high wavelengths, between 3000 cm^{-1} and 3400 cm^{-1} showed a broad and strong band stretch, indicative of the presence of $–NH_2$ groups and free or hydrogen bonded O–H groups [29]. The narrow peaks at 2920.61 cm^{-1} and 2851.54 cm^{-1} showed the asymmetric C–H bond of methyl and methylene groups [30] and N–H vibration, respectively. The peak at 1772.19 cm^{-1} can be attributed to unionized C-O stretching of the carboxylic acid. The peak at 1650.97 cm^{-1} was attributed to COO−, C=O and C–N peptidic bond of proteins [31]. The

peak at 1455.12 cm^{-1}, was correlated with the symmetric bending of CH_3 [32]. The bands at 1211.16 cm^{-1} might be attributed to phosphonate (P–OH) group stretching [33,34]. The bands appearing between 950 and 1200 cm^{-1} might be attributed to C-O group stretching [32]. We noticed that peaks at 1211.16, 1772.29, 285.54 and 2920.61 cm^{-1} are strong for H_3PO_4-MSK. It can be thereby noted that the IR spectrum of the powdered MSK and H_3PO_4-MSK supported the presence of O–H, COOH, C = O, C–N, C–H, C-O, $–NH_2$ and P–OH as functional groups. The diversity of functional groups indicated the presence of cellulose, lignin, starch and proteins [30].

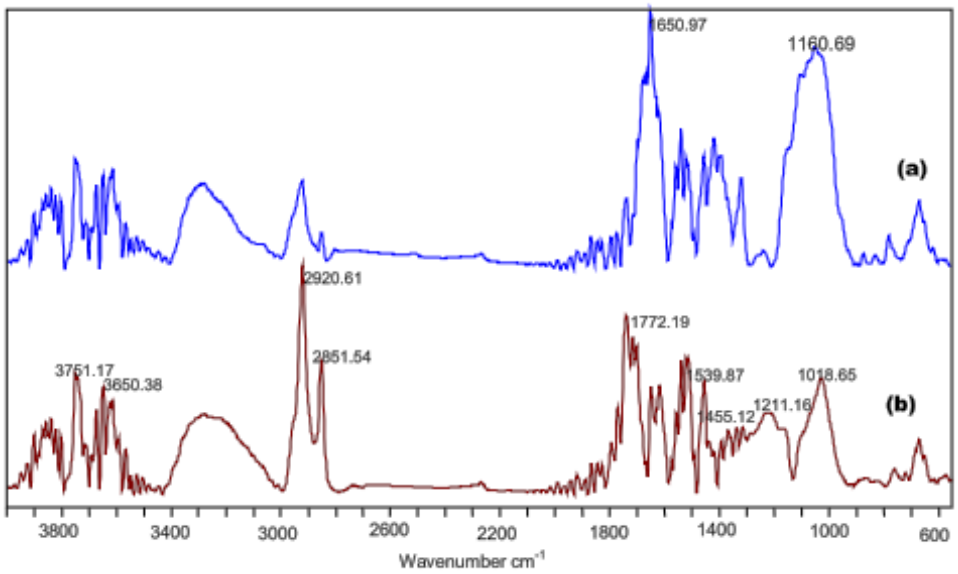

Figure 4. FTIR spectra of (a) crude MSK and (b) H_3PO_4-MSK.

Point of zero charge and pH influence. The pH where, the sum of charges at the surface of an adsorbent are equal to zero, is generally known as the point of zero charge (pH_{PZC}). The pH_{PZC} of H_3PO_4-MSK is 5.4 as presented in the Fig. 5. At pH > pH_{PZC} the adsorbent is negatively charged and the adsorbed species are positively charged. Such a situation improves the electrostatic attraction between the adsorbate and the negatively charged surface of the adsorbent. At pH < pH_{PZC} the surface of the adsorbent is positively charged.

Data presented in the Fig. 6 show the influence of the pH on the CV adsorption onto H_3PO_4-MSK. The adsorbed amount presents two major domains. When the pH is between 3 and 8 the adsorbed amount increased,

while when the pH is higher than 8 the adsorbed amount decreased. The increase of the amount adsorbed with the pH indicates a weak electrostatic attraction during the adsorption process. If the electrostatic attraction was strong, we would have had an interruption of the evolution of the amount adsorbed at pH 5.4 which is the point of zero charge. This situation is unfavorable for electrostatic attraction. This increase of the adsorbed amount suggests that the adsorption could also involve surface complexation.

The formed complex might be instable at pH greater than 8, which leads to the decrease oh the adsorbed amount [36].

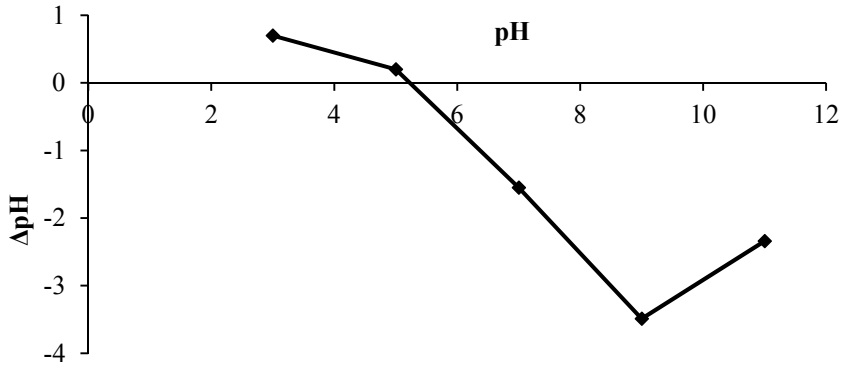

Figure 5. H_3PO_4-MSK point of zero charge.

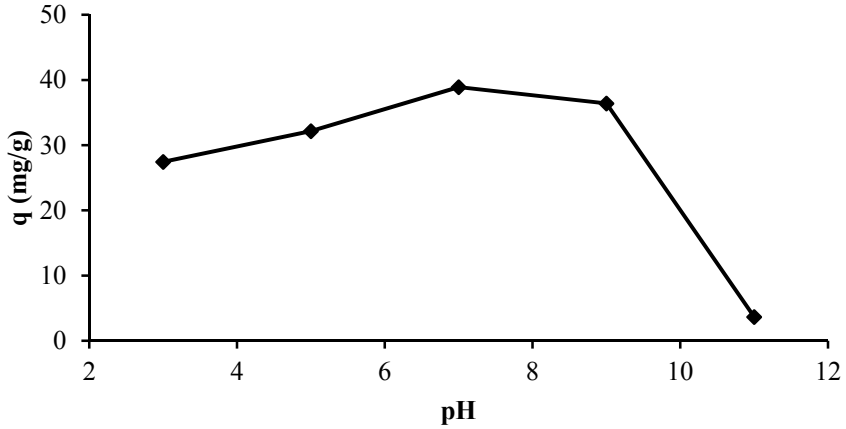

Figure 6. Effect of the pH on the CV adsorption on H_3PO_4-MSK.
(50 mg/L, 25°C, 0.1g, 240 min)

Kinetic studies

Effect of adsorbent quantity. The adsorption of CV is relatively fast in the first 50-100 min, then the adsorption rate decreases and progresses much slower thereafter towards the equilibrium (240 min), irrespective to the adsorbent quantity, (Fig. 7). The amount of CV adsorbed per gram of adsorbent, decreases as the adsorbent quantity increases (Fig 7a). This shows that surface diffusion became rate-determining step due to particle agglomeration, which leads to difficult access to the adsorption sites. The relative amount of CV adsorbed at equilibrium is 78, 85 and 93% for 0.1, 0.2 and 0.3 g of adsorbent, respectively (Fig 7b). This indicates that a better efficiency will be obtained if CV solution would be treated successively with 0.1 g of adsorbent than one step treatment with 0.3 g of adsorbent.

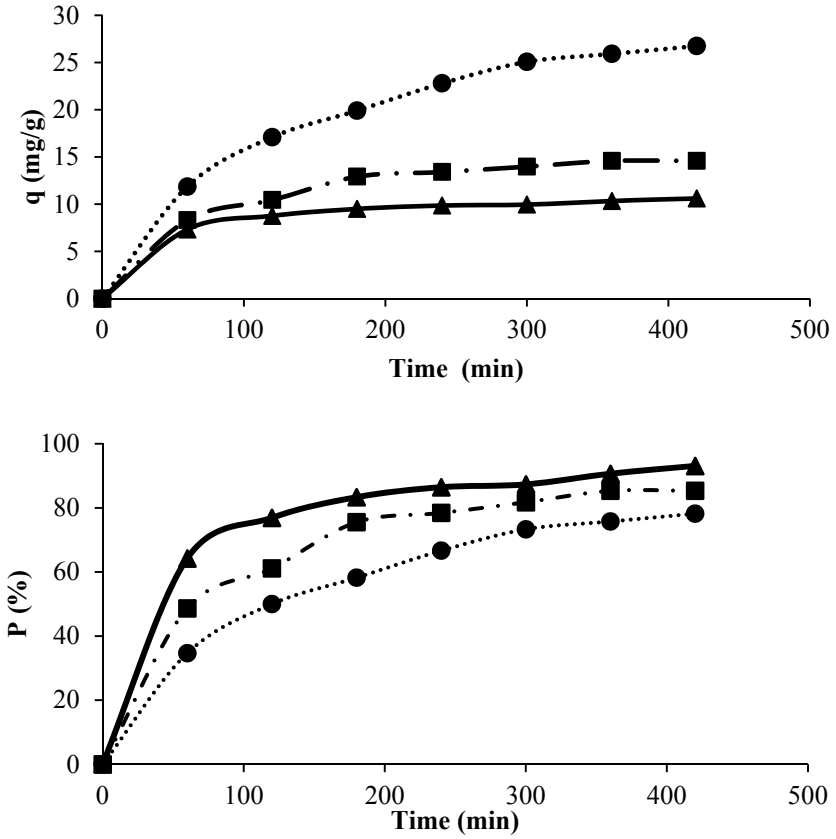

Figure 7. Adsorption kinetics of CV onto H_3PO_4-MSK (a) adsorbed amount and (b) relative amount adsorbed, for different adsorbent quantities, ●0.1 g, ■0.2 g and ▲0.3 g (50 mg/L, 25°C, pH 6).

Kinetic modeling. In order to analyze the adsorption kinetics of CV, the pseudo-first- and pseudo-second-order and simple Elovich models were applied to the experimental data.

The pseudo-first-order rate equation or Lagergren equation is derived on the assumption of one step reaction [37] and is expressed as:

$$\ln(q_e - q_t) = \ln q_e - k_1 t \tag{3}$$

where, q_e is the amount of dye adsorbed at equilibrium (mg/g), q_t is the amount of dye adsorbed at time t (mg/g), k_1 is the pseudo-first-order reaction rate constant (1/min).

Pseudo-second-order equation based on two step reaction is usually expressed in the form [38,39]:

$$\frac{t}{q_t} = \frac{1}{k_2 q_e^{\,2}} + \frac{t}{q_e} \tag{4}$$

where, k_2 is the pseudo-second-order reaction rate equilibrium constant (g/mg·min).

The simple Elovich model may be expressed in the form:

$$q_t = A + B \ln t \tag{5}$$

where, A and B (mg/g·min) are Elovich constants, related to the initial adsorption rate and to the number of available site for adsorption. B is related to the extent of surface coverage and activation energy for chemisorption.

Based on the fact that pseudo-second-order equation is derived on the assumption of a two-step reaction, we concluded that CV adsorption takes place as a two-step reaction scheme. The pseudo-second-order model is build based on the assumption that the rate-controlling step is chemical adsorption involving valence force by sharing or exchange of electrons between adsorbent and adsorbate [40]. Therefore, a satisfactory fitness of this model suggested that chemisorption was the rate-controlling step [41]. A and B parameters derived from Elovich equation are used to estimate the reaction rates. It was suggested that an increase in A value and/or decrease in B value would increase the rate of the adsorption process. The obtained R^2 values for H_3PO_4-MSK for all the dosage were high, suggesting that Elovich model describes this adsorption system.

The estimated model and the related statistic parameters for CV adsorption onto H_3PO_4-MSK are presented in Table 2. Based on linear regression analysis, correlation coefficient (R^2) values, we concluded that the kinetics of CV onto the considered adsorbent is well described by pseudo-second-order and Elovich models. The amount of adsorbed CV

determined from the two mentioned equations fitted very well with the experimental values (Table 2).

The negative value of k_1 indicated that the pseudo-first-order model cannot be applied to describe the adsorption of CV on H_3PO_4-MSK.

Intra-particle diffusion. The common diffusion model usually designated as intra particle model is expressed as [42]:

$$q_t = k_{int} t^{1/2} + D \quad (6)$$

where, k_{int} is the intra-particle diffusion rate constant (mg/L·min$^{1/2}$) and D the constant. The fitting of the experimental data with this model was checked using so-called Weber and Morris plot of q versus $t^{1/2}$. According to intra-particle diffusion model, a plot of uptake, q versus the square root of time, $t^{1/2}$, should be linear if intra-particle diffusion is involved in the adsorption system and if this line passes through the origin, then intra-particle diffusion is the rate controlling step [43]. In this study, the relative plot of q and $t^{1/2}$ obtained for Crystal Violet dye adsorption on H_3PO_4-MSK did not go through the origin. Also it was indicative of some degree of boundary layer control and this further indicated that the intra-particle diffusion was not the only rate controlling step; other mechanisms were simultaneously operating during the adsorption of CV on H_3PO_4-MSK.

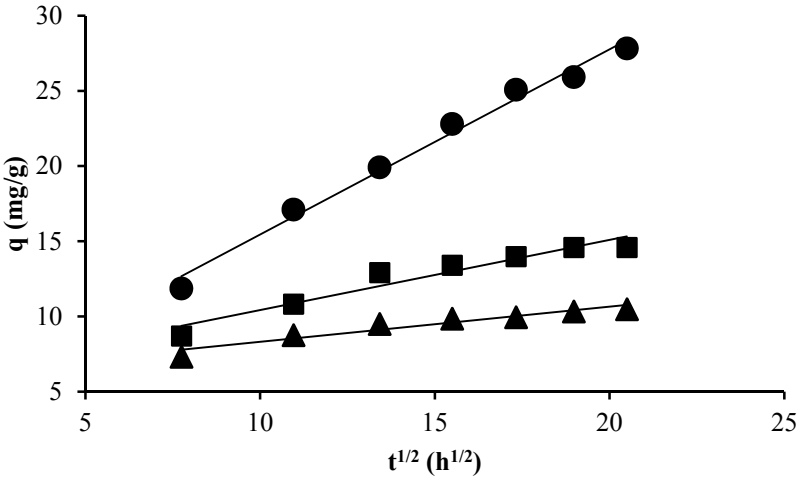

Figure 8. Intra-particle diffusion model for CV adsorption onto H_3PO_4-MSK, for different adsorbent quantities, ●0.1 g, ■0.2 g and ▲0.3 g (50 mg/L, 25°C, pH 6).

Table 2. Kinetic parameters for the adsorption of CV onto H_3PO_4-MSK (50 mg/L, 25°C, pH 6); q_{exp} and q_{cal} are the experimental and calculated amount of CV adsorbed per gram of adsorbent

Kinetic models	Parameters	Experiment		
		0.1 g	**0.2 g**	**0.3 g**
Pseudo-first-order	q_{exp} (mg/g)	22,80	13,40	9,80
	$k_1 \times 10^{-2}$ (1/min)	-0.15	-0.07	-0.06
	q_e (mg/g)	38.53	25.39	15.50
	q_{cal} (mg/g)	22.61	11.17	7.22
	R^2	0.9748	0.8744	0.8633
Pseudo-second-order	$k_2 \times 10^{-2}$ (min·g/mg)	0.70	1.70	3.00
	q_e (mg/g)	0.52	0.53	0.57
	q_{cal} (mg/g)	23.16	13.47	9.87
	R^2	0.9956	0.9987	0.9960
Elovich	A	-21.92	-4.10	1.01
	B	8.17	3.17	1.59
	q_{cal} (mg/g)	22.87	13.25	9.73
	R^2	0.99	0.99	0.99
Intra-particle diffusion	k_{int} (1/min)	1.23	0.47	0.23
	D	3.14	5.75	5.98
	q_{cal} (mg/g)	22.21	12.98	9.6
	R^2	0.9955	0.9782	0.9776

Equilibrium studies

Isotherm modeling. Adsorption isotherms modeling are prerequisites to understand the nature of the interaction between adsorbate and the adsorbent. In order to successfully represent the equilibrium adsorption behavior, it is important to have a satisfactory description of the equation state between the two phases of the adsorption system. Three well known phenomenological equations were tested to fit the experimental data, namely Langmuir, Freundlich and Temkin equations [42,44]. They are expressed as follows:

$$\text{Langmuir equation: } \frac{1}{q_e} = \frac{1}{q_{max} K_L} \cdot \frac{1}{C_e} + \frac{1}{q_{max}} \tag{7}$$

$$\text{Freundlich equation: } \ln q_e = \ln K_F + \frac{1}{n} \ln C_e \tag{8}$$

$$\text{Temkin equation: } q_e = B \ln A + B \ln C_e \tag{9}$$

where q_e, q_{max} and C_e, are, the amount adsorbed at equilibrium (mg/g), the amount adsorbed at the monolayer (mg/g) and the equilibrium concentration of CV (mg/L), respectively. K_L is the Langmuir adsorption equilibrium constant (L/mg), K_F is the Freundlich constant related to the adsorption capacity ($mg^{(1-1/n)}\ L^{1/n}/g$) and n is the Freundlich constant related to the adsorption energy. B is Temkin constant related to adsorption energy (J/mol) and A is the Temkin constant (L/mg).

Considering the correlation coefficient (R^2) values, Table 3, the following series was obtained for CV adsorption onto H_3PO_4-MSK: Langmuir > Temkin > Freundlich. The adsorption of CV on H_3PO_4-MSK is favorable as n takes value in the range of 1 to 10. However, the small value of B indicates that CV is loosely bond to H_3PO_4-MSK, therefore the adsorption is physical in nature. The essential characteristic of Langmuir isotherm can be expressed in terms of dimensionless separation factor of equilibrium parameter, R_L, defined by the equation [44]:

$$R_L = \frac{1}{1 + K_L C_0} \tag{10}$$

where, C_0 is the highest dye concentration in solution (mg/L). The values of R_L indicates the type of isotherm to be irreversible (R_L=0), favorable (0<R_L<1), linear (R_L=1) or unfavorable (R_L>1). The calculated value of R_L for the highest concentration of 300 mg/L obtained for H_3PO_4-MSK indicates (Table 3) that is a suitable adsorbent for CV removal from aqueous solutions.

Table 3. Isotherms parameter values for the adsorption of CV onto H_3PO_4-MSK (50-300 mg/L, 0.1 g, pH 6).

Isotherm models	Constants	Values
Langmuir	K_L (L/mg)	0.38
	q_{max} (mg/g)	112.44
	R_L	0.0087
	R^2	0.9907
Freundlich	K_F ($mg^{(1-1/n}\ L^{1/n}/g$)	34.48
	n	2.40
	R^2	0.9474
Temkin	A (L/mg)	34.93
	B (J/mol)	21.72
	R^2	0.9849

Fig. 9 shows the plot of the amounts of CV adsorbed versus equilibrium dye concentrations. The amount of dye adsorbed increased from 23.94 to 87.25 mg/g for an increase in initial dye concentration from 50-300 mg/L, whereas the percent dye removal decreases from 79 to 33% for an increase in initial dye concentration from 50-300 mg/L. The adsorption isotherm has the L form considering Giles classification [45].

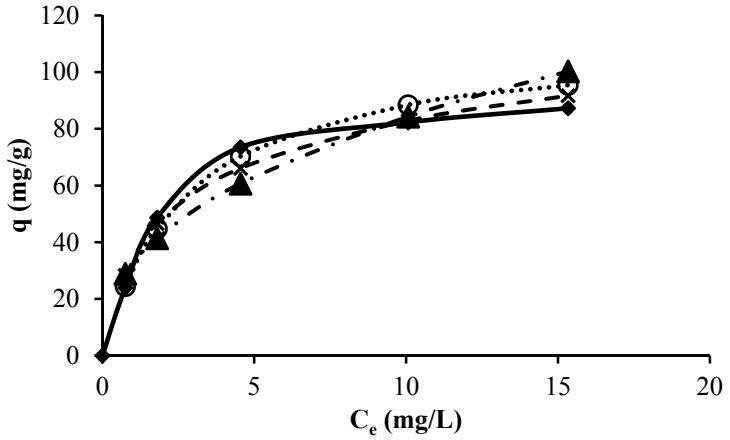

Figure 9. Isotherms of CV adsorption onto H_3PO_4-MSK (♦Experimental values, ○Langmuir, ▲Freundlich; ×Temkin).

Thermodynamics

Effect of temperature. Experiments were performed at different temperatures 30, 40 and 50°C for the initial concentration of 50 mg/L. The CV adsorbed amount (mg/L) increases as temperature increases (Fig. 10). The results showed that the adsorption was endothermic in nature. Since adsorbent is porous and CV diffusion in pores plays an important role in the adsorption process, increase in the adsorption with the rise of temperature may be diffusion controlled, which is an endothermic process, i.e. the rise of temperatures favors the CV transport within the pores of the adsorbent. The increased adsorption with the rise of temperature is also due to the increase in the number of the adsorption sites generated because of the breaking of some internal bonds near the edge of the active surface sites of the adsorbent [46,47].

Thermodynamic parameters. Standard thermodynamic parameters such as change in free energy (ΔG°), enthalpy (ΔH°) and entropy (ΔS°) were calculated using the following equations:

$$K_c = \frac{C_a}{C_e} \tag{11}$$

$$\Delta G^\circ = -RT\ln K_c \tag{12}$$

$$\ln K_c = -\frac{\Delta H^\circ}{RT} + \frac{\Delta S^\circ}{R} \tag{13}$$

where, K_c is the equilibrium constant, C_a and C_e are the equilibrium concentration (mg/L) of CV on the adsorbent and in solution, respectively, T is the temperature (K) and R is the universal gas constant (kJ/K·mol). $\Delta H°$ and $\Delta S°$ were obtained from the slope and the intercept of van't Hoff plot of $\ln K_c$ versus 1/T and values are presented in Table 4. The negative free energy values indicate that the adsorption process is spontaneous. It was also noted a decrease in the free energy values with an increase in temperature corresponding to an increase of the adsorbed CV amount. The positive values of the enthalpy further confirm the endothermic nature of the process whereas the positive values of entropy reflect good affinity of the dye towards H_3PO_4-MSK [48,49]. When the CV is adsorbed on the surface of the adsorbent, water molecules previously bonded to the dye cation are released and dispersed in the solution, which leads to the increase of the entropy [50].

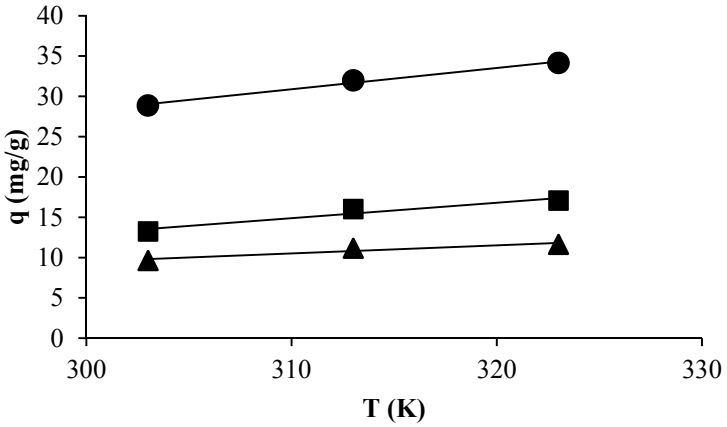

Figure 10: Effect of temperature on the adsorption of CV onto H_3PO_4-MSK at 25°C, 50mg/L, time 240 min, pH 6 (●0.1g, ■0.2g and ▲0.3g).

Table 4. Thermodynamic parameters for CV adsorption onto H_3PO_4-MSK.

Samples	R^2	Temperature (K)	ΔG° (kJ/mol)	ΔH° (J/mol)	ΔS° (J/mol·K)
0.1 g	0.96	303	-4.19	142.86	482.95
		313	-6.79		
		323	-13.94		
0.2 g	0.98	303	-3.07	170.06	569.41
		313	-6.88		
		323	-14.55		
0.3 g	0.98	303	-3.20	185.29	622.28
		313	-7.55		
		323	-14.34		

Adsorption mechanism

The binding mechanisms of dyes by adsorption could be explained by the physical and chemical interactions between cell wall ligands and adsorbates by ion exchange, complexation, coordination and micro-precipitation. The diffusion of the dye from the bulk solution to active sites of the adsorbents occurs predominantly by passive transport mechanisms, while various functional groups such as carboxyl, hydroxyl, amino and phosphate existing on the cell wall can bind the dye molecules. The adsorption dynamics can be described by the following three consecutive steps, which are as follows [22]: transport of the dye molecules from bulk solution through the liquid film to the adsorbent exterior surface, migration on the adsorbent surface and diffusion into the pore of the adsorbent, and adsorption on the interior pores surfaces of the adsorbent.

The last step is considered to be an equilibrium reaction. Out of three steps, the third step is assumed to be rapid. Therefore, the adsorption of CV onto H_3PO_4-MSK is probably controlled by a two-step reaction scheme. The adsorption of CV onto H_3PO_4-MSK was proposed to take place according to the following chemical mechanism:

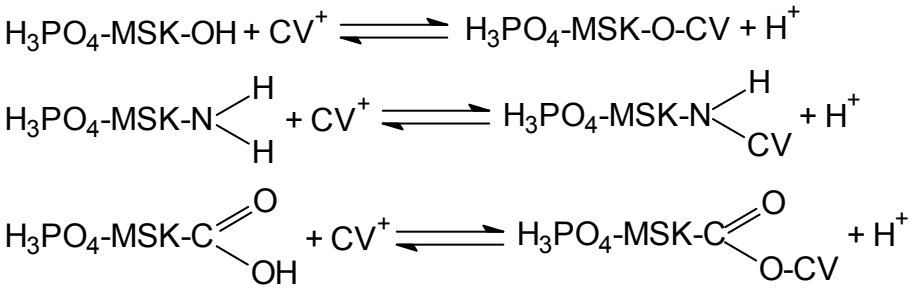

CONCLUSION

The ability of H_3PO_4-MSK to retain dyes with high molecular weight was investigated for CV dye using kinetic, equilibrium and thermodynamic models. The kinetics of CV onto H_3PO_4-MSK was studied using the pseudo-first-order, pseudo-second-order and Elovich kinetic models. The results indicated that the pseudo-second-order and Elovich models provided the best correlation with the experimental data. Then, CV adsorption rate is governed by two-step reaction scheme. The adsorption process followed well Temkin and Langmuir models. Calculated thermodynamic parameters

indicated that the adsorption in this system was a spontaneous and endothermic process. These results suggest that H_3PO_4-MSK is a potential low-cost adsorbent for dye removal from industrial wastewaters.

EXPERIMENTAL

Material

Mango seeds kernel (MSK) used as adsorbent in this study was collected from Ngaoundere a city, in the Adamawa Region, Cameroon. MSK was treated by concentrated phosphoric acid (H_3PO_4), then washed with deionized water and dried at 110°C for 24 h. The dried H_3PO_4-MSK was grounded to fine powder and sieved to a particle size < 50µm.

Crystal Violet (CV) dye was of commercial grade (M_F: $C_{25}H_{30}N_3Cl$, M_W: 408, λ_{max}: 586 nm) and it was used without further purification (Fig. 11). Stock solution was prepared by dissolving 1g of the CV powder in 1000 mL distilled water. For adsorption experiments this solution was diluted to the desired initial concentrations ranging from 50-300 mg/L. The initial solution pH was adjusted to the desired value by adding drop wise HCl, 0.1M or NaOH, 0.1M solutions.

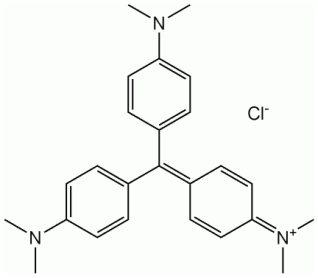

Figure 11. Structural formula of Crystal Violet.

Adsorbent characterization

Elemental analysis (C, H, N, S) was performed using a CHN CARLO ERBA EA 1108 Elemental Analyzer. The oxygen percentage was estimated by difference.

The thermal behavior of the H_3PO_4-MSK sample was studied using a TGA/SDTA 851, 1600°C Mettler-Toledo analyzer. Experimental conditions were as follows: initial mass of the sample was 18.91 mg, initial temperature 25°C, final temperature 800°C, heating rate of 10°C/min and nitrogen flow of 50 mL/min. The DTG and TG curves were obtained by calculating the derivative simultaneously.

The X-ray diffraction (XRD) was used to determine the crystalline structure of the H_3PO_4-MSK sample. The X-ray diffractograms were obtained at room temperature within a 2θ ranging from 5 to 40 and a scan rate of 1°/min. The equipment used was a Bruker Advance D8 diffractometer, operating at a power of 40 kV with a current of 30 mA and Cu Kα radiation (1.5406 Å). Before performing the analysis the sample was dried at 50°C for 12 h in an air-circulating oven.

The surface structure of H_3PO_4-MSK was analyzed using Scanning Electron Microscopy (SEM Quanta 2000 - Philips) at an electron acceleration voltage of 25 kV. Prior to scanning, the unloaded and dye-loaded H_3PO_4-MSK sample was mounted on a stainless steel stab with double stick tape and coated with a thin layer of gold in a high vacuum condition.

Infrared spectra were recorded using a Nicolet Magna FT-IR-750 spectrometer thoroughly mixing MSK and H_3PO_4-MSK with KBr matrix.

Specific surface area and pore specific volume for the H_3PO_4-MSK were determined by the Brunauer–Emmett–Teller (BET) method using a Sorptomatic ADP-nitrogen adsorption analyzer (Thermo Electron-Corp.). Prior to N_2 adsorption, samples were out gazed for 20 h at 105°C.

The pH of the point of zero charge (pH_{pzc}) corresponds to the pH were the sum of all the electrical charges at the surface of the adsorbent are equal to zero. pH_{pzc} determination method consist in the preparation of a solution of desired pH in the 2-11 range. HCl 0,01M solution was dropwise to a 50 mL NaCl 0,01M solution until de pH value was reached. 0,05 g of adsorbent were then added to the prepared solution. The mixture is then stirred at 50 rpm for 24 h. The pH of the solution is noted and the graph of the pH versus the variation of the pH is drawn. The value at the intersection of the obtained curve with the x-axis gives the pH_{pzc} of the adsorbent [51].

Batch adsorption experiments

A predetermined amount of H_3PO_4-MSK was added into 100 mL conical flasks filled with 25 mL of CV solution of known concentration. The flasks were then placed in a shaking water bath (50 cycles/min) at room temperature for 24 hours. The samples were then withdrawn at predetermined time interval and the residual concentration of CV was determined by UV-Visible spectroscopy. The absorbance was measure at 586 nm with 1 cm optical path length quartz cell. TG Instrument T-70 UV-Vis spectrophotometer was used for this purpose. The concentration of CV was determined from the calibration curve.

The adsorbed amount of CV per gram of adsorbent (q, in mg/g) and the relative amount adsorbed (P, in %) were expressed as:

$$q = (C_0 - C_f) \cdot \frac{V}{m} \quad (1)$$

$$P = \frac{C_0 - C_f}{C_0} \cdot 100 \quad (2)$$

where, C_o is the initial concentration of CV (mg/L), C_f is the final concentration of CV (mg/L), V is the volume of the solution (L) and m the amount of adsorbent (g).

Statistical analysis

In order to ensure the accuracy and reliability, all experiments were performed in triplicate, and the mean values were used in data analysis. Relative standard deviations were found to be within ±3%. Microsoft Office Excel program was employed for data processing. Linear regression analysis was employed to fit experimental data with theoretical models.

ACKNOWLEDGEMENTS

This work was carried out with financial support from the Romanian Ministry of Foreign Affairs and the Agence Universitaire de la Francophonie, Bureau of Central and Eastern Europe (BECO), Bucharest, Romania. Ghislain Arnaud MOUTHE ANOMBOGO wish to express sincere thanks to the Romanian Government for the Fellowship "EUGEN IONESCU" offered.

REFERENCES

1. J. Atchana, G.M. Simu, S.G. Hora, M.E. Grad, J.B. Tchatchueng, B.L. Benguellah, R.Kamga, *Journal of Food, Agriculture & Environment*, **2011**, *9*, 457.
2. G. Bogoeva-Gaceva, A. Bužarovska, B. Dimzoski, *G. U. Journal of Science*, **2008***, 21*, 123.
3. A. Aygun, T. Yilmaz, *International Journal of Chemical and Environmental Engineering*, **2010**, *1*, 97.
4. H. Valdes, H.P. Godoy, C.A. Zaror, *Journal of International Association of Water Pollution Research,* **2010**, *61*, 2973.
5. F-R. Xiu, F-S. Zhang, *Journal of Hazardous Materials*, **2009**, *172*, 1458.
6. A.R. Khataee, M. Fathinia, S. Aber, M. Zarei, *Journal of Hazardous Materials*, **2010**, *181*, 886.

7. U. Singh, R.K. Kaushal, *International Journal of Technical & Non-Technical Research*, **2013**, *4*, 33.
8. G.Z. Kyzas, F. Jie, K. A. Matis, *Materials*, **2013**, *6*, 5131.
9. M.A. Mohammed, A. Shitu, M. A. Tadda, M. Ngabura, *International Research Journal of Environment Sciences*, **2014**, *3*, 62.
10. R. Kamga R., G.J. Kayem, P.G. Rouxhet, *Journal of Colloid and Interface Science,* **2000**, *232*, 198.
11. J.B. Bike Mbah, R. Kamga, J. P. Nguetnkam, J. Fanni, *European Journal of Lipid Science and Technology,* **2005**, *107*, 387.
12. A. Bhatnagar, A. K. Minocha, *Indian Journal of Technology*, **2006**, *13*, 203.
13. G. Bayramoglu, B. Altintas, M. Yakup Arica, *Chemical Engineering Journal*, **2009**, *152*, 339.
14. G. Crini, *Journal of Biotechnology*, **2006**, *97*, 1061.
15. L.S. Oliveira, A.S. Franca, in "Food Science and Technology: New Research" L.V. Greco, M.N. Bruno, editors, Nova Publishers, New York, **2008**, chapter 3.
16. A.E. Ofomaja, *Chemical Engineering Journal*, **2008**, *143*, 85.
17. D. Park,Y-S. Yun, J.M. Park, *Biotechnology and Bioprocess Engineering*, **2010**, *15*, 86.
18. M.P. Elizalde-Gonzalez, V. Hernandez-Montoya, *Biochemical Engineering Journal*, **2007**, *36*, 230.
19. A.S. Franca, L.S. Oliveira, P.I.A. Santos, S.A Saldanha., S.A. Salum, *Journal of Biotechnology*, **2008**, *136*, S655.
20. M.M. Davila-Jimenez, M.P. Elizalde-Gonzalez, V. Hernandez-Montoya, *Bioresource Technology*, **2009**, *100*, 6199.
21. T. Murugan,A. Ganapathi, R. Valliappan, *E-Journal of Chemistry*, **2010**, *7*, 669.
22. K.K. Vasanth, A. Kumaran, *Biochemical Engineering Journal,* **2005**, *27*, 83.
23. FAO report, "Situation actuelle et perspectives à moyen terme pour les fruits tropicaux", FAO Data Base, **2004**.
24. E.B. Djantou Njantou, "Optimisation du broyage des mangues séchées (Manguifera indica var Kent): Influence sur les propriétés physicochimiques et fonctionnelles des poudres obtenues", Thèse de Doctorat PhD, INP de Lorraine et Université de Ngaoundéré*,* **2006**.
25. G.G Stavropoulos., A.A. Zabaniotou, *Microporous and Mesoporous Materials*, **2005**, *82*, 79.
26. M.T Uddin, M. Rukanuzzaman, M.M.R. Khan, M.A. Islam*, Journal of Environmental Management*, **2009**, *90*, 3443.
27. M.A. Henrique, H.A. Silvério, W.P. Flauzino Neto, D. Pasquini, *Journal of Environmental Management*, **2013**, *121*, 202.
28. W.P. Flauzino Neto, H.A. Silverio, N.O. Dantas, D. Pasquini, *Industrial Crops and Products*, **2013**, *42*, 480.
29. C.J. Duran-Valle, M. Gomez-Corzo, J. Pastor-Villegas, V. Gomez-Serrano, *Journal of Analytical and Applied Pyrolysis*, **2005**, *73*, 59.
30. A. Saeed, M. Sharif, M. Iqbal, *Journal of Hazardous Materials*, **2010**, *179*, 564.
31. O. Gulnaz, A. Kaya, S. Dincer, *Journal of Hazardous Materials*, **2006**, *134*, 190.
32. A. Khaled, A.E. Nemr, A. El-Sikaily, O. Abdelwahab, *Journal of Hazardous Materials*, **2009**, *165*, 100.

33. X.N. Li, Q.Y. Xu, G.M. Han, W.Q. Zhu, Z.H. Chen, X.B. He, *Journal of Hazardous Materials*, **2009**, *165*, 469.
34. S. Sadhasivam, S. Savitha, K. Swaminathan, F. H. Lin, *Journal of the Taiwan Institute of Chemical Engineering*, **2009**, *40*, 394.
35. W. Jianlong, Z. Xinmin, D. Decai, Z. Ding, *Journal of Biotechnology*, **2001**, *87*, 273.
36. G. Mckay, Y.S. Ho, *Process Biochemistry*, **1999**, *34*, 451.
37. R. Ansari, Z. Mosayebzadeh, A. Mohammad-Khah, *Journal of Advanced Scientific Research,* **2011**, *2*, 25.
38. P.D. Saha, S. Chakraborty, S. Chowdhury, *Colloids and Surfaces B: Biointerfaces*, **2012**, *92*, 262.
39. D.K. Mahmoud, M.A. Mohd Salleh, W.A.W. Abdul Karim, A. Idris, Z.Z. Abidin, *Chemical Engineering Journal*, **2012**, *181-182*, 449.
40. I. Kula, M. Ugurlu, H.C. Karaoglu, A. Elik, *Bioresource Technology*, 2008, *99*, 492–501.
41. Y.S. Ho, G. McKay, *Water Research,* **2000**, *34*, 735–742.
42. R. Ahmad, *Journal of Hazardous Materials***,** 2009, *171*, 767.
43. W.T. Tsai, K.J. Hsien, J.M. Yang, *Journal of Colloid and Interface Science*, **2004**, *275*, 428–433.
44. K. Porkodi, K.K. Vasanth, *Journal of Hazardous Materials*, **2007**, *143*, 311.
45. G. Limousin, J.P. Gaudet, L. Charlet, S. Szenknect, V. Barthes, M. Krimissa, *Applied Geochemistry*, **2007**, *22*, 249.
46. S. Chakraborty, S. Chowdhury, P. D. Saha, *Carbohydrate Polymers*, **2011**, *86*, 1533.
47. P.D. Saha, S. Chakraborty, S. Chowdhury, *Colloids and Surfaces B: Biointerfaces*, **2012**, *92*, 262.
48. H.C. Chu, K.M. Chen, *Process Biochemistry,* **2002**, *37*, 1129.
49. R.K. Gautam, A. Mudhoo, M.C. Chattopadhyaya, *Journal of Environmental Chemical Engineering,* **2013**, *1*, 1283.
50. S. Senthilkumaar, P. Kalaamani, C. V. Subburaam, *Journal of Hazardous Materials*, **2006**, *136*, 800.

P.C.C. Faria, J.J.M. Orfao, M. F. R. Pereira, Water Resources, **2004**, *38*, 2043.